

Regional Analysis for an Economically and Environmentally Viable Transition to Heavy-Duty Vehicles with Alternative Powertrains

Author, co-author (Do NOT enter this information. It will be pulled from participant tab in MyTechZone)

Affiliation (Do NOT enter this information. It will be pulled from participant tab in MyTechZone)

Abstract

The transportation sector is responsible for a significant portion of greenhouse gas emissions. Within the sector, truck freight is responsible for a third of the associated emissions. Alternative powertrains are seen as a viable approach to significantly reduce these emissions. Prior to making a large-scale transition, it is important to consider the following questions: will the power grid support a transition to alternative powertrains?; will the transition truly reduce carbon emissions?; and will the transition impose an unnecessary economic burden on companies within the industry? The answer to these questions, however, can vary by geography, maturity/capacity of the energy distribution network or predicted vehicle load. We focus on the latter two questions, investigating the variation in estimated total cost of ownership and carbon emissions across the United States at the zip code level for both heavy-duty battery electric vehicles and heavy-duty fuel cell electric vehicles. As a benchmark, we compare estimated emissions and costs of alternative powertrain vehicles to that of conventional heavy-duty vehicles powered by diesel internal combustion engines. This work highlights areas with electric grids primed for a transition to alternative powertrain vehicles, such as the Pacific Northwest, and areas that require further infrastructure investment in renewables, such as many of the Mountain states, Missouri, and Florida. Additionally, this work illustrates the current advantages in carbon emissions of battery electric vehicles compared to fuel-cell electric vehicles, while providing insights into required regional investments for narrowing the gap.

Introduction

In the U.S., heavy-duty vehicles (HDVs) are 10% of vehicles on roadways, yet they account for almost 28% of CO₂ emissions from highway vehicles [1]. This makes alternative energy sources an important avenue to reduce the environmental impact of HDVs. However, the transition must be done with awareness of the added costs and of the potential for reducing carbon emissions, to ensure change is sustainable economically and offers a net positive environmental benefit. The cost competitiveness and carbon reduction potential varies depending on region, influenced by factors such as energy costs, infrastructure availability, and regional grid carbon intensity [2]. It is crucial to assess these regional variations to ensure that the transition to alternative powertrains is both economically viable and environmentally beneficial across the United

States. This study aims to provide a techno-economic comparison of the estimated total cost of ownership (TCO) and expected carbon emissions for conventional diesel HDVs, heavy-duty battery electric vehicles (BEVs), and heavy-duty fuel cell electric vehicles (FCEVs) across the 48 contiguous United States. By doing so, it offers insights into where and how the adoption of BEVs and FCEVs can be most effectively implemented. We follow this up with an investigation into the sensitivity of pricing and emissions due to different parameters, with the hope of aiding stakeholders in making future decisions.

There has been a global push to transition HDVs to zero-emission vehicles (ZEVs) due to their out-sized contribution to greenhouse gas emissions. One such effort is the Global Commercial Vehicle Drive to Zero, a global memorandum endorsed by 37 countries, including the United States, that commits to a goal of transitioning to 30% ZEV new HDV sales by 2030 and 100% ZEV new HDV sales by 2040 [3]. Furthermore, regulations like the Advanced Clean Fleet (ACF) initiative require a 100% transition to zero-emission vehicles for on-road vehicles over 8,501 lbs Gross Vehicle Weight Rating (GVWR) by 2042. For commercial fleet operators and government policymakers, developing a strategic decarbonization plan is essential to successfully navigate and implement this transition.

As we move towards this ambitious goal, it becomes imperative to focus on both the economic and environmental aspects of this transition. Cost and carbon emissions are two of the most significant factors influencing the adoption of alternative powertrains in the heavy-duty sector. Understanding these factors in the context of regional variability allows us to identify where alternative powertrains can be most beneficially deployed. This study specifically addresses these issues by comparing the TCO and carbon emissions of BEV and FCEV HDVs to that of diesel HDVs across different regions, thus highlighting the areas that are most suitable for early adoption and those that may require more infrastructure support or policy incentives. We focus on BEVs and FCEVs here, because the powertrains have zero tailpipe carbon emissions. However, we acknowledge that other low-carbon alternative powertrains exist.

Prior research in the field of HDVs has predominantly concentrated on economic analysis, examining factors such as fuel efficiency, maintenance costs, and lifecycle emissions. Several studies have investigated the economic aspects of HDVs, focusing primarily on fuel efficiency and its impact on operating costs. These studies have shown that improving fuel efficiency can significantly reduce the TCO for HDV operators. For instance, the work in [4] explored

various factors influencing fuel consumption, such as vehicle design and engine technology. Other research highlights how advancements in aerodynamics and engine efficiency contribute to lower fuel consumption and overall cost savings [5]. Maintenance costs have also been a crucial component of economic analysis for HDVs. Studies indicate that transitioning to electric HDVs can reduce maintenance expenses due to fewer moving parts and the absence of exhaust systems, which are commonly associated with traditional diesel engines [6]. Furthermore, lifecycle emissions analysis reveals that electric HDVs offer substantial reductions in greenhouse gas and criterion emissions compared to their diesel counterparts, thus presenting significant environmental benefits [7]. Studies have highlighted the need for detailed regional analyses to better understand the economic and environmental implications of transitioning to electric vehicles. For example, [8] emphasizes the importance of considering local factors such as electricity grid composition, climate, and driving patterns to better understand the economic and environmental implications of transitioning to electric vehicles. Regional analyses help identify areas where electric HDVs can provide the most benefits and where additional infrastructure investments may be needed [9,10]. However, there remains a gap in comprehensive studies that simultaneously address both cost and carbon metrics at a national scale.

The objective of this study is to gain insights into what regions across the U.S. are most (or least) suited for a transition to heavy-duty BEVs and FCEVs from economic sustainability and environmental impact perspectives. This paper contributes to the existing body of work by providing a detailed analysis of the TCO and carbon emissions for HDVs, offering a unique perspective on regional differences across the United States due to the energy source's cost and carbon intensity. Additionally, it includes a sensitivity analysis that examines how changes in energy pricing, battery or fuel cell costs, and grid carbon intensity might impact the competitiveness and environmental benefits of BEVs and FCEVs. This analysis aims to inform stakeholders, including policymakers, industry leaders, and researchers, to make informed decisions regarding the transition to electric HDVs.

The remainder of this paper is organized as follows: We first describe the methodology used to estimate the TCO and carbon emissions for diesel, battery electric and fuel cell electric HDVs. Next, we present the results, highlighting regional variations and the implications for BEV and FCEV adoption. This is followed by a sensitivity analysis that explores the impact of various parameters on the cost and carbon emissions of BEVs and FCEVs. Finally, we discuss the findings and their implications for stakeholders, concluding with recommendations for future research and policy directions.

Methods

Both total cost of ownership and carbon emissions depend on the efficiency of the truck variant. Despite the dependence of efficiency on the route (including speeds traveled, accelerations, elevation change, ambient temperatures, etc.) and, therefore, the region the HDV is operating in, we assume a constant efficiency across the nation for simplicity. Future work is focused on estimating efficiency variation across regions. According to the North American Council for Freight Efficiency (NACFE), the 2021 estimate for average fuel economy for conventional diesel internal combustion engine (ICE) HDVs is 6.49 miles per diesel gallon equivalent (mpdge) [11]. We consider this efficiency for the current state or standard (std.) diesel HDVs. To account for future technological enhancements, we assume

enhanced (enh.) diesel HDVs operate with the average efficiency from the two NACFE Run on Less demonstrations (2017 and Regional in 2019), or 9.15 mpdge [11]. These assumptions are optimistic as the average efficiency for all U.S. trucks in 2020 was 6.24 mpdge [11]. However, the more stringent baseline of the higher performing systems and ideal operators from the NACFE campaigns provide some level of confidence the qualitative takeaways will hold into the future.

For alternative powertrains, we also consider both the current state, or std., and future state due to technological developments, or enh., heavy-duty BEVs and FCEVs. For the std. HD BEV, we use the results of the NACFE Run on Less Electric demonstration from 2021 for Class 8 terminal tractors, or 2.88 kWh/mi [12]. As there is not significant data on the current state of HD FCEV efficiency, the std. HD FCEV is assumed to be 7.5 mi/kg H₂, or the upper bound on efficiencies observed in the literature from [13]. For the enh. variants of the HD BEVs and FCEVs, it is assumed that the same technological advancements (e.g. those that reduce aerodynamic drag or rolling resistance) that improved the diesel HDVs efficiency may be applied. Therefore, we scale the efficiency of the std. alternate powertrains by the ratio of std. diesel-ICE to enh. diesel-ICE efficiency (or ~1.41) to obtain the enh. HD BEV and FCEV efficiencies. The efficiency values for all powertrain variants are summarized in Table 1. For reference and easy comparison across architectures, the efficiency in mpdge and consumption in kWh/mi are provided for all powertrains. We note that the enh. HD BEV consumption of 2.04 kWh/mi is in the range of the U.S. Department of Energy (DOE) funded SuperTruck 3 project [14,15]. While the enh. HD FCEV efficiency of 10.57 mi/kg H₂ are conservative and align with the lower end of the U.S. DOE 2030 predictions for HD FCEVs [16].

Table 1. Assumed efficiency of vehicle variants. Green shading indicates the native units for the given powertrain.

Powertrain Variant	Efficiency		
	mpdge	kWh/mi	mi/kg H ₂
Diesel-ICE	Std.	6.49	5.75
	Enh.	9.15	4.08
BEV	Std.	12.96	2.88
	Enh.	18.30	2.04
FCEV	Std.	8.33	4.48
	Enh.	11.74	3.18

Next, we discuss how total cost of ownership is approximated across the nation, followed by the processes for estimating carbon emissions.

Total Cost of Ownership

In this report, the method for estimating TCO presented in [17] is adopted, where the TCO (C_{TCO}) in \$/mi comprises capital investments, operational and maintenance costs, as well as end-of-life and environmental impact expenses. For the details with respect to each cost, the reader is directed to [17]. Here, we assume the TCO can be separated into two components: the energy cost C_E and the rest of the ownership costs (including capital investment, operations, maintenance, etc. for both the vehicle and infrastructure) C_{rest} , i.e. $C_{TCO} = C_E + C_{rest}$. Although costs (including acquisition, operational, maintenance and others) may vary by region, we assume C_{rest} is uniform across the country for simplicity. As part of future work, this assumption may be relaxed and the variation in C_{rest} may

be considered. To estimate C_{rest} , we average the TCO of 6 representative trucks with high annual vehicle miles traveled (VMT) from [17] and then subtract out the fuel expense. The resulting constant $C_{rest} = 1.26$ \$/mi for diesel trucks, 1.99 \$/mi for both BEVs, and 1.44\$/mi for both FCEVs. These values are on a similar order of TCO values less fuel expense found in [18].

Alternatively, the energy cost is assumed to vary across the nation, where $C_{E,ijx} = C_{fuel,ix}/\eta_{ij}$ for each HDV powertrain $i \in \{diesel, BEV, FCEV\}$, subvariant $j \in \{std., enh.\}$, and each region x in the nation. The efficiency $\eta_{ij} = a_i \eta_{ij,0}$ of each variant is the product of the efficiency values in mpdge from Table 1 designated $\eta_{ij,0}$ and a conversion constant a_i to bring the energy units into agreement with the cost ($a_{diesel} = 1$, $a_{BEV} = 0.027$ dge/kWh, and $a_{FCEV} = 0.9$ dge/kg H₂ [19]). The fuel cost $C_{fuel,ix}$ of region x and HDV i is the average cost per gallon (\$/gal) for diesel, the average cost per kilowatt (\$/kWh) of electricity for BEVs, and the average cost per kg H₂ (\$/kg H₂) for FCEVs. For diesel pricing, data for gas stations in each zip code was pulled from GasBuddy.com [20] in late April of 2024 for consumer diesel and averaged over the zip code. While for electricity pricing, the 2023 average commercial rates by zip code from the National Renewable Energy Laboratory (NREL) hosted on OpenEI.org [21] are used.

As hydrogen is not widely available across the country for the transportation sector, historical data on its pricing does not exist. To fill this gap, we investigate three pathways to hydrogen production: grid electrolysis, electrolysis with Energy Attribute Credits (EACs) [22] or Renewable Energy Certificates (RECs) [23], and electrolysis using distributed solar energy. The grid electrolysis pathway is seen as a corner case and in general inadvisable, however, looking at regional variations may give insight into unique regions where it is viable. The EACs/RECs pathway explores how a uniform net rate discount across the nation may impact viability of using grid power, while local solar electrolysis provides regional insights into a potential low carbon pathway and where it may be viable. We acknowledge further hydrogen pathways exist and may be the more likely path forward, exploring additional pathways is part of future work.

For an initial investigation, we assume hydrogen is produced in each region, i.e. with energy from that region. However, we note that in reality hydrogen may be produced in favorable regions and distributed elsewhere, which is a focus of future work. For grid electrolysis, the hydrogen cost predictions are based on the commercial electricity rates from OpenEI.org. While for electrolysis with EACs/RECs, the commercial electricity rates are assumed to have a net reduction of \$0.05/kWh for each region due to sale of associated EACs/RECs. We acknowledge that this is highly speculative but provides valuable insight into how a net rate decrease may impact pricing across the nation. Lastly, the cost of distributed solar power for solar electrolysis is adopted from [24] based on the Renewable Energy Potential Model (reV) [25] and the Annual Technology Baseline [26].

The cost of hydrogen under the assumption of grid electrolysis is:

$$C_{fuel,FCEVx} = \left[\left(\frac{LHV_{H_2}}{\eta_{H_2,elec}} \right) + E_{comp} \right] C_{electricity,px} + C_{H_2,rest}, \quad (1)$$

where LHV_{H_2} is the lower heating value of hydrogen, $\eta_{H_2,elec}$ is the efficiency of producing hydrogen from electrolysis (assumed to be

70% here), $E_{comp} = 5.56$ kWh/kg H₂ (obtained from [27]) is the energy required for compression, $C_{electricity,px}$ is the cost of electricity in \$/kWh for region x using the pathway $p \in \{grid, EAC / REC, solar\}$, and $C_{H_2,rest}$ encompasses additional costs associated with production, distribution, and dispensing (e.g. capital expenses, etc.). For this study, $C_{H_2,rest} = 2.4$ \$/kg H₂ assuming 8 dispensers and a type C or D hourly demand distribution as described in [28]. We note that $C_{H_2,rest}$ may vary depending on the capacity factor of the electrolyzer pathway, which will be investigated in future work.

Although the above energy pricing data is provided with respect to zip codes, a zip code is used to represent a mail route from the post office and not a geographic area [29]. The U.S. Census Bureau developed zip code tabulation areas (ZCTAs) to represent generalized geographic areas occupied by zip code routes [29]. In order to be consistent with mapping and our discussion based on geographic distributions, we use the Geocorr 2022 application from the Missouri Census Data Center [30] to obtain the correlation between zip codes and ZCTAs. If there are multiple zip codes associated with a given ZCTA, the fuel cost (either for diesel, electricity, or hydrogen prices) for the ZCTA is assumed to be an average of the zip codes contained within it. If no data on fuel cost exists for a given ZCTA (i.e. there was no data for the associated zip codes), we use the average fuel cost of all neighboring ZCTAs. With fuel cost data available for all ZCTAs, the TCO is calculated for each ZCTA x , powertrain i , and variant j as $C_{TCO,ijx} = C_{E,ijx} + C_{rest,i}$. For reference, Figure 1 provides the maps of fuel costs, $C_{fuel,ix}$, for each energy source.

Total Carbon Emissions

The predicted well-to-wheel carbon emissions of a region for an HDV variant $m_{CO_2,ijx} = I_{ix}VMT_x/\eta_{ij}$ is the product of the carbon intensity I_{ix} for the fuel of powertrain i , efficiency η_{ij} of the variant j of powertrain i (see Table 1) and vehicle-miles-traveled VMT_x of region (or ZCTA) x . We assume all VMT in a region can be transitioned to the alternative powertrain to gain insight into the potential of BEVs and FCEVs. Future work will address feasibility limitations due to range as well as other aspects dependent on use case.

The carbon intensity (kg CO₂/gal) for diesel HDVs is considered constant across the nation for this study. The carbon emitted from burning diesel is 10.18 kg CO₂/gal [31], while the carbon emissions associated with transportation from the point of manufacture to the dispensing station are 1.89 kg CO₂/gal [27], resulting in a total carbon intensity for diesel of 12.07 kg CO₂/gal. In reality, the transportation emissions will vary by region. Incorporating this variation is a focus of future work.

The carbon intensity of the BEV variants are considered to be the same carbon intensity as the grid. At the county level, data on the electricity generation source is pulled from the U.S. Energy Information Administration's (EIA) Open Data API for the year 2023 [32], then the county grid carbon intensity I_{ix} in kg CO₂/kWh is a weighted combination of carbon intensity of generation sources. The source carbon intensity is also obtained from EIA [32]. The grid carbon intensity for a ZCTA is considered to be equivalent to the carbon intensity of the county it lies in. The correlation from county to ZCTA is obtained using data from Geocorr 2022 [30]. If the ZCTA is within multiple counties, the carbon intensity is taken as the average carbon intensity of the counties it lies within.

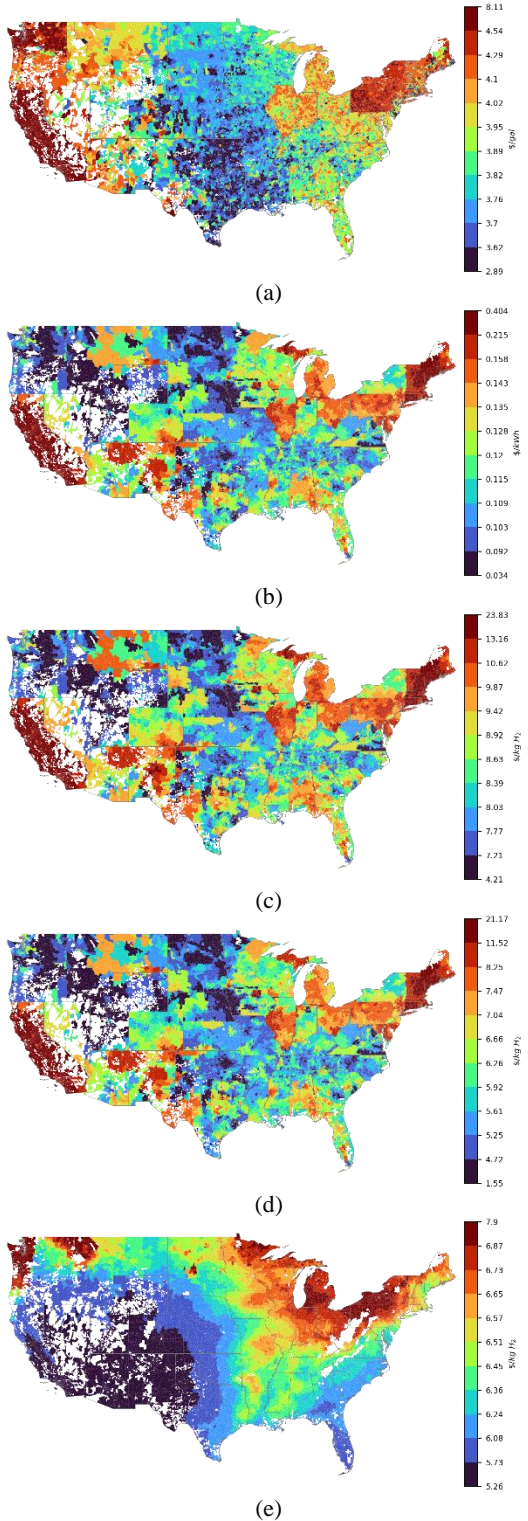


Figure 1. Energy pricing by ZCTA for (a) consumer diesel, (b) commercial electricity, and hydrogen from electrolysis using (c) current local grid power, (d) EAC/REC local grid power, and (e) local distributed solar. Hydrogen pricing assumes the hydrogen is produced in each region, more competitive pricing may be achieved by producing in favorable regions and distributing elsewhere.

Lastly, under the assumption that hydrogen is produced locally by electrolysis, the carbon intensity of hydrogen is then:

$$I_{FCEVx} = I_{electricity,px} \left(\frac{LHV_{H_2}}{\eta_{H_2elec}} + E_{comp} \right), \quad (2)$$

where $I_{electricity,px}$ is the carbon intensity of the $p \in \{grid, solar\}$ electricity pathway used for electrolysis. For the case of local grid electrolysis, the above data on grid carbon intensity [32] is used for $I_{electricity,px}$. Whereas, for local solar electrolysis regional data from [24] on solar panel area ($A_{PV,x}$) and average annual energy production (AEP_x) by region are used along with (3) to approximate the local carbon intensity of solar energy.

$$I_{electricity,solarx} = \frac{I_{PV} A_{PV,x}}{L_{PV} AEP_x}. \quad (3)$$

The carbon intensity of a solar panel is assumed to be $I_{PV} = 125$ kg CO₂/m² [27], with an assumed life $L_{PV} = 30$ years. This resulted in a range of 25 to 47 g CO₂/kWh depending on location, which is within the range published by NREL [33]. We drop the EAC/REC pathway for carbon intensity analysis, due to a lack of currently available data. Future work can investigate the availability of EACs and RECs for different energy sources by region.

The last input required to obtain the expected carbon emissions $m_{CO_2,ijx}$ for a ZCTA in kg CO₂ is the VMT_x . The VMT at the county level is pulled from the Freight Analysis Framework [34]. To obtain an approximation of the VMT at the ZCTA level, the county level VMT is distributed based on the percentage of primary and secondary roads within the county that lie within the ZCTA. The length of primary and secondary roads within a ZCTA are obtained from the National Neighborhood Data Archive [35]. The length of primary and secondary roads within a county is then the sum of the length of primary and secondary roads within each ZCTA in the county. If a ZCTA is within multiple counties, the primary and secondary roads are assumed to be evenly distributed across the counties.

To summarize, the inputs into our analysis are zip code level diesel, electricity and hydrogen costs, efficiencies for the three HDV variants, a representative TCO without fuel costs, correlation between zip codes, ZCTAs and counties, carbon intensity for diesel and the electric grid, county level VMT for freight, and the length of primary and secondary roads within each ZCTA. Table 2 presents the associated values and variables for constants within the regional analysis (except for vehicle efficiency already in Table 1).

Table 2. Additional constants utilized in the analysis of TCO and carbon emissions.

Name	Variable	Diesel	BEV	FCEV
Rest cost	C_{rest} (\$/mi)	1.26	1.99	1.44
Electrolysis additional costs	C_{H_2rest} (\$/kg H ₂)	—	—	2.4
Hydrogen lower heating value	LHV_{H_2} (kWh/kg H ₂)	—	—	33.3
Electrolysis efficiency	η_{H_2elec}	—	—	0.7
Energy for H ₂ compression	E_{comp} (kWh/kg H ₂)	—	—	5.56
Diesel carbon intensity	I_{diesel} (kg CO ₂ /gal)	12.07	—	—
Carbon intensity of a solar panel	I_{PV} (kg CO ₂ /m ²)	—	—	125
Life of a solar panel	L_{PV} (years)	—	—	30

Results and Discussion

We first analyze the regional variations in estimated TCO, followed by a discussion on the predicted change in carbon emissions associated with a 100% transition to alternative powertrains. We conclude the results with an investigation into the sensitivity of these findings to changes in electricity rates, and battery costs.

Total Cost of Ownership

To illustrate the potential changes in TCO associated with a transition to alternative powertrains, Figure 2 through Figure 5 map the reduction in TCO for the alternative powertrains ($C_{TCO,diesel,kx} - C_{TCO,ijx}$, $\forall i \in \{BEV, FCEV\}$, $j, k \in \{std., enh.\}$, $x \in \text{all ZCTA}$). Figure 2 presents the results comparing BEVs to diesel. Based on the assumptions within this paper, the std. BEV is not competitive from a cost perspective with diesel, as nowhere within the US has a predicted lower TCO, with the majority of the regions having an increase in TCO of 0.40 \$/mi or more than the std. diesel (see Figure 2(a)). It is, however, important to note that with the exception of parts of California and New England, the majority of the nation has a predicted increase in TCO for std. BEVs less than 0.73 \$/mi, which is the difference in $C_{rest,diesel}$ and $C_{rest,BEV}$. This means that in general fuel costs for the std. BEV are lower and if other investments and operating costs can be reduced, then the std. BEV could be competitive. Considering efficiency improvements for both BEV and diesel powertrains in Figure 2(d), realizes a larger increase in the predicted TCO for the enh. BEV compared to the enh. diesel. This is because the fuel expense is a larger portion of the diesel TCO than the BEV TCO resulting in a greater impact of efficiency improvements for the enh. diesel. Despite this, much of the nation still sees a TCO increase less than 0.73 \$/mi. Figure 2(b) and (c) have been included to show how TCO may be impacted if efficiency improvements in the diesel or the BEV, respectively, outpaces improvements in the other powertrain. For example, Figure 2(c) could be a result of improvements in battery technology that would not be transferable to the diesel powertrain.

The general regional trends in Figure 2(a) to (d) are consistent. First, the Pacific Northwest is the closest for BEVs to be competitive with diesel from a cost perspective, particularly in Central Washington. This is due to relatively high diesel prices and low electricity rates (Figure 1(a) and (b)). The next regions that are closest to BEV competitiveness with diesel are North Dakota and the four Atlantic states: North Carolina, eastern Virginia, West Virginia and New York. Again, this is due to relatively high diesel costs compared to their electricity prices (Figure 1(a) and (b)). More specifically, North Dakota, North Carolina, eastern Virginia and West Virginia have low electricity rates and moderate diesel prices, while New York has moderate electricity rates and high diesel prices.

On the other end of the spectrum are the five regions with the highest increase in TCO associated with a transition to BEVs, including portions of the southern Mountain state (northeast Arizona, central New Mexico, and southeast Colorado), northwestern Iowa, the Upper Peninsula of Michigan, much of California, and New England. The southern Mountain States, northwestern Iowa, and the upper Peninsula of Michigan have particularly high electricity rates and moderately low diesel prices, causing the significant increase in TCO (Figure 1(a) and (b)). Whereas, California and New England have moderately high diesel prices (Figure 1(a)), yet their electricity rates are still significantly higher (Figure 1(b)), driving the TCO increase.

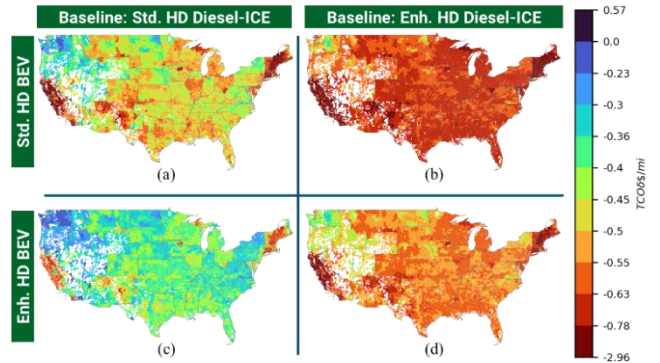


Figure 2. Maps of the reduction in TCO ($C_{TCO,diesel,kx} - C_{TCO,ijx}$, $\forall j, k \in \{std., enh.\}$) for std. BEV compared to (a) std. and (b) enh. diesel, as well as, for enh. BEV compared to (c) std. and (d) enh. diesel. The primary focus is on (a) and (d) where like variants are compared. However, (b) and (c) have been included to gain insight into variations associated with either the diesel or BEV powertrain, respectively, increasing efficiency while the other remains stagnant. Positive values (darkest blue) mean the alternative powertrain has a lower predicted TCO than diesel.

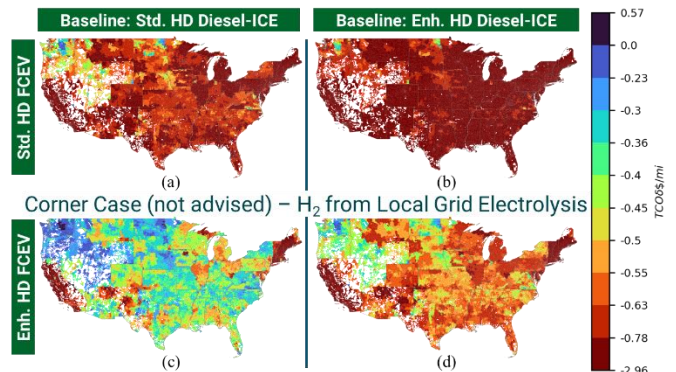


Figure 3. Maps of the reduction in TCO ($C_{TCO,diesel,kx} - C_{TCO,FCEV,ijx}$, $\forall j, k \in \{std., enh.\}$) for std. FCEV compared to (a) std. and (b) enh. diesel, as well as, for std. FCEV compared to (c) std. and (d) enh. diesel assuming hydrogen is produced from electrolysis using current local grid power. The primary focus is on (a) and (d) where like variants are compared. However, (b) and (c) have been included to gain insight into variations associated with either the diesel or FCEV powertrain, respectively, increasing efficiency while the other remains stagnant. Positive values (darkest blue) mean the alternative powertrain has a lower predicted TCO than diesel. As expected, for the majority of the U.S. hydrogen produced from local grid electrolysis is not competitive, with the exception of the Pacific Northwest where electricity rates are low and diesel is expensive.

Figure 3 presents the same comparisons for FCEVs using hydrogen from electrolysis using local grid energy. This is not expected to be a viable direction forward for widespread adoption. The regional variations in all four maps of Figure 3 mirror those in Figure 2 as the underlying variation is due to grid electricity rates (see (1)). Unlike with the BEV powertrain, however, when comparing Figure 3(a) (std. FCEV to std. diesel) to Figure 3(d) (enh. FCEV to enh. diesel), the increase in TCO compared to diesel reduces. This is because the fuel costs for FCEVs using hydrogen from local grid electrolysis is a more significant portion of their TCO. From a cost perspective, there are two regions where local grid electrolysis may be viable: first is in central Washington, where electricity costs are particularly low and diesel prices are particularly high; second is in northeast North

Dakota, where electricity prices are low and diesel prices are moderate.

As supported by Figure 3, hydrogen produced by local grid electrolysis is not expected to be widely viable. To see how a uniform net reduction in electricity rates (for example by the use and sale of EACs/RECs), we present Figure 4 comparing FCEVs using locally produced hydrogen with electrolysis using EACs/RECs. Again, regional trends mirror the underlying grid electricity costs. With a net 0.05 \$/kWh reduction (equivalent to a 2.66 \$/kg H₂ reduction) the increase in TCO compared to diesel has come down to less than 0.55 \$/mi for std. variants (Figure 4(a)) and less than 0.4 \$/mi for enh. variants (Figure 4(d)). If efficiency improvements for the FCEV were to outpace that of the diesel HDV (e.g. by improvements to the fuel cell that would not be reflected in the diesel powertrain), the majority of the nation only has an increase of 0.23 \$/mi or less, with many regions in the Pacific Northwest, West North Central, Mountain states seeing a reduction in TCO compared to diesel (see Figure 4(c)). Another notable observation from Figure 4 is that even if diesel efficiency improvements outpaced that of FCEV efficiency improvements (see Figure 4(b) comparing std. FCEV to enh. diesel), there are locations in central Washington and a small region in North Dakota where FCEVs are predicted to have lower TCO than diesel. Although the scenario considering electrolytic hydrogen locally produced using EACs/RECs is highly speculative, it shows that there may be viable pathways for FCEVs to be competitive with diesel through a reduction in hydrogen costs.

The hydrogen pathways with local production through electrolysis using grid power or EACs/RECs have been dependent on the underlying grid electricity rates, therefore, the regional trends more or less follow that of the BEV (compare Figure 3 and 4 to Figure 2). A more likely hydrogen pathway using electrolysis is using behind-the-meter renewable energy, e.g. through solar. Figure 5 presents the reduction in TCO maps comparing FCEVs using hydrogen from local solar electrolysis. Remembering Figure 1, the regional trends observed in the four maps in Figure 5 are primarily driven by the regional trends in the cost of solar (Figure 1(e)). There is an exception in northern Atlantic regions (such as New England and New York) where high diesel prices have made the FCEV variants using hydrogen from local solar electrolysis more competitive than expected by the solar energy cost map (Figure 1(e)).

Comparing the maps in Figure 5 to those in Figure 3 and 4, we see that local solar electrolysis results in less regional variation in reduction in TCO compared to the other two hydrogen pathways. As an example, Figure 5(a) comparing std. FCEVs and std. diesel HDVs has an increase in TCO ≤ 0.55 \$/mi, where a few regions in California where the predicted TCO for FCEVs is less than that of diesel. California is the most cost competitive region with low solar energy costs and high diesel prices for FCEVs using hydrogen from local solar electrolysis. This is converse to scenarios with local electrolysis using grid and EACs/RECs, where California has expensive electricity and therefore expensive hydrogen through electrolysis. The trends comparing efficiency variants (moving from Figure 5(a) to (b), (c), or (d)) are similar to those observed in Figure 3 and 4.

Comparing Figure 4 and 5 highlights the need to explore various hydrogen pathways depending on region. As previously mentioned, California is not cost competitive for FCEVs when considering hydrogen from local electrolysis with EACs/RECs (Figure 4), while when considering hydrogen from local solar electrolysis it is cost competitive (Figure 5). Similarly, the Pacific Northwest is more cost

competitive for FCEVs considering hydrogen from local electrolysis with EACs/RECs (Figure 4) than considering hydrogen from local solar electrolysis it is cost competitive (Figure 5). The three explored hydrogen pathways are also not the only potential pathways. Therefore, future work is focused on exploring regional variations for additional pathways to determine which pathways are competitive by region. Later, we explore the carbon implications of some of the further hydrogen pathways (as seen in Table 4). Another important consideration that is not explored here, is the fact that hydrogen is dispatchable, i.e. hydrogen can be produced in one region and distributed out to neighboring regions. Future work will explore leveraging regions with viable and cost competitive hydrogen pathways to produce low-cost hydrogen for distribution to neighboring higher cost regions.

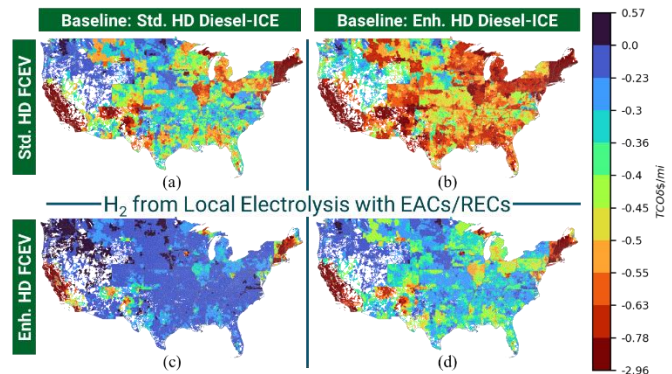


Figure 4. Maps of the reduction in TCO ($C_{TCO,diesel,kx} - C_{TCO,FCEV,jx}$, $\forall j, k \in \{\text{std.}, \text{enh.}\}$) for std. FCEV compared to (a) std. and (b) enh. diesel, as well as, for std. FCEV compared to (c) std. and (d) enh. diesel assuming hydrogen is produced from local electrolysis using EACs/RECs. However, (b) and (c) have been included to gain insight into variations associated with either the diesel or FCEV powertrain, respectively, increasing efficiency while the other remains stagnant. Positive values (darkest blue) mean the alternative powertrain has a lower predicted TCO than diesel.

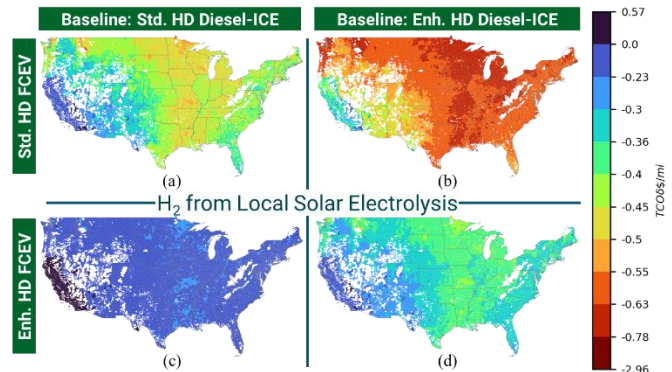


Figure 5. Maps of the reduction in TCO ($C_{TCO,diesel,kx} - C_{TCO,FCEV,jx}$, $\forall j, k \in \{\text{std.}, \text{enh.}\}$) for std. FCEV compared to (a) std. and (b) enh. diesel, as well as, for std. FCEV compared to (c) std. and (d) enh. diesel assuming hydrogen is produced from electrolysis using distributed local solar power. However, (b) and (c) have been included to gain insight into variations associated with either the diesel or FCEV powertrain, respectively, increasing efficiency while the other remains stagnant. Positive values (darkest blue) mean the alternative powertrain has a lower predicted TCO than diesel.

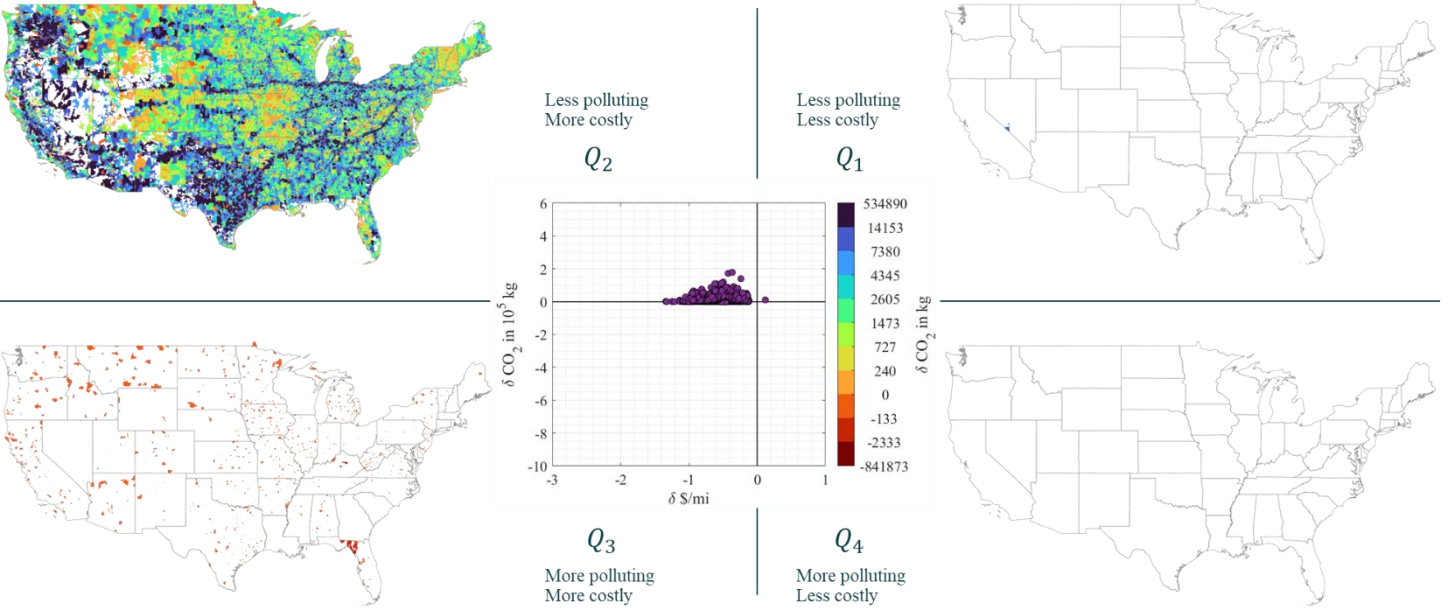


Figure 6. In the center is a scatter plot of the predicted reduction in kg CO₂ emissions (δCO_2) vs. reduction in TCO per mile ($\delta\$/\text{mi}$) of each ZCTA resulting from a transition to *std. BEVs* from *std. diesel HDVs*. Each quadrant has a map of the reduction in kg CO₂ for the data points in that quadrant. The regions scattered throughout the U.S. in orange that occur in both Q_2 and Q_3 have no VMT data (i.e. $VMT = 0$).

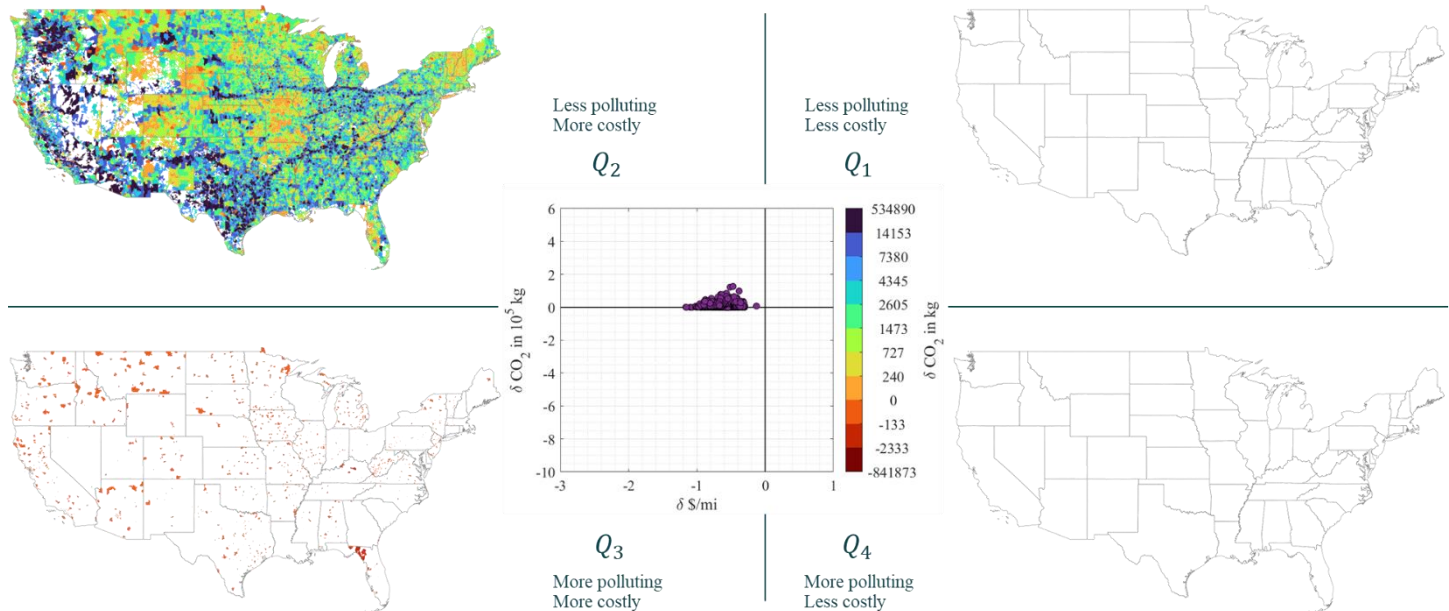


Figure 7. In the center is a scatter plot of the predicted reduction in kg CO₂ emissions (δCO_2) vs. reduction in TCO per mile ($\delta\$/\text{mi}$) of each ZCTA resulting from a transition to *enh. BEVs* from *enh. diesel HDVs*. Each quadrant has a map of the reduction in kg CO₂ for the data points in that quadrant. The regions scattered throughout the U.S. in orange that occur in both Q_2 and Q_3 have no VMT data (i.e. $VMT = 0$).

Total Carbon Emissions

Next, we explore the carbon emissions implications associated with a 100% transition to alternative powertrains by evaluating the predicted reduction in emissions of kg CO₂ in each region ($m_{CO_2,diesel x} - m_{CO_2,ijx}$, $\forall i \in \{BEV, FCEV\}, j \in \{std., enh.\}, x \in \text{all ZCTA}$). For this section, we consider only hydrogen locally produced with solar electrolysis as hydrogen through local grid electrolysis is not commercially viable (as shown in the prior section) and we do not have regional data for the carbon emissions implications of EACs/RECs.

Page 7 of 14

Table 3. Summary of quadrant designations.

Quadrant designation	Reduction in kg CO ₂	Reduction in TCO
Q_1	>0	>0
Q_2	>0	<0
Q_3	<0	<0
Q_4	<0	>0

In the center of Figure 6 is a scatter plot of the reduction in carbon emissions (δCO_2) versus the reduction in TCO ($\delta\$/\text{mi}$) for *std. BEVs*. Outside each quadrant is a map of the corresponding data

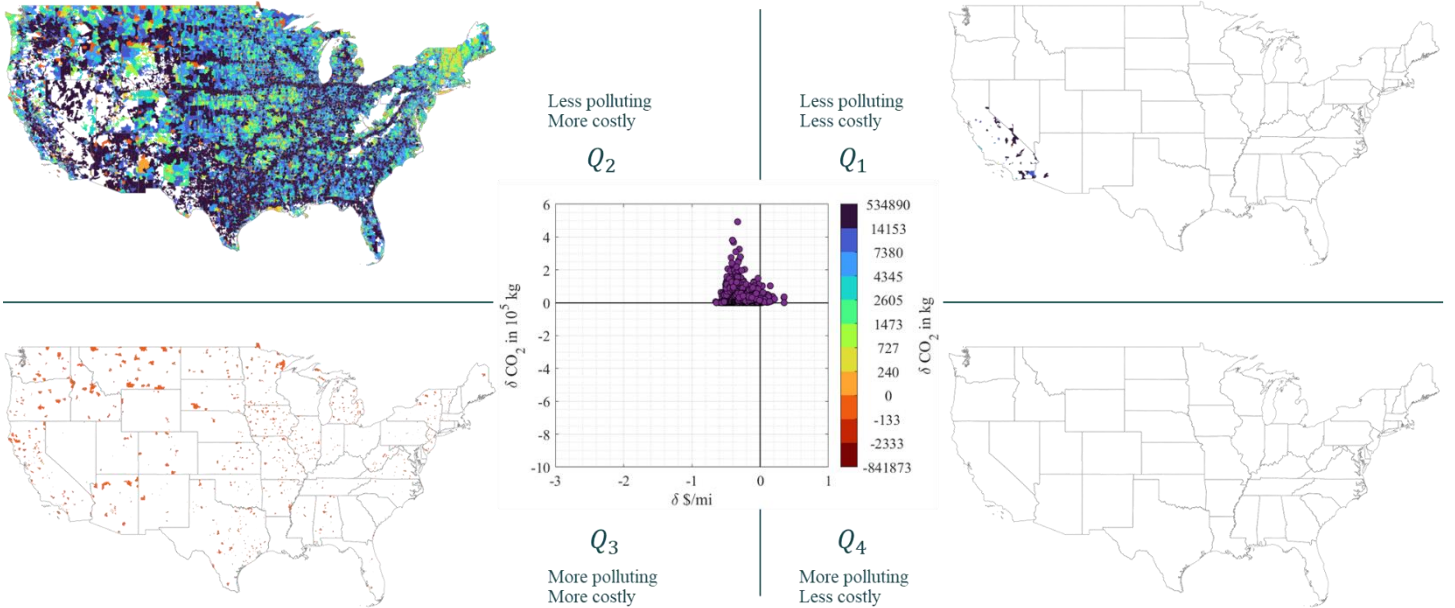


Figure 8. In the center is a scatter plot of the predicted reduction in kg CO₂ emissions (δCO_2) vs. reduction in TCO per mile ($\delta\$/\text{mi}$) of each ZCTA resulting from a transition to *std. FCEVs* from *std. diesel HDVs* using electrolytic hydrogen produced from local solar power. Each quadrant has a map of the reduction in kg CO₂ for the data points in that quadrant. The regions scattered throughout the U.S. in orange that occur in both Q_2 and Q_3 have no VMT data (i.e. $VMT = 0$).

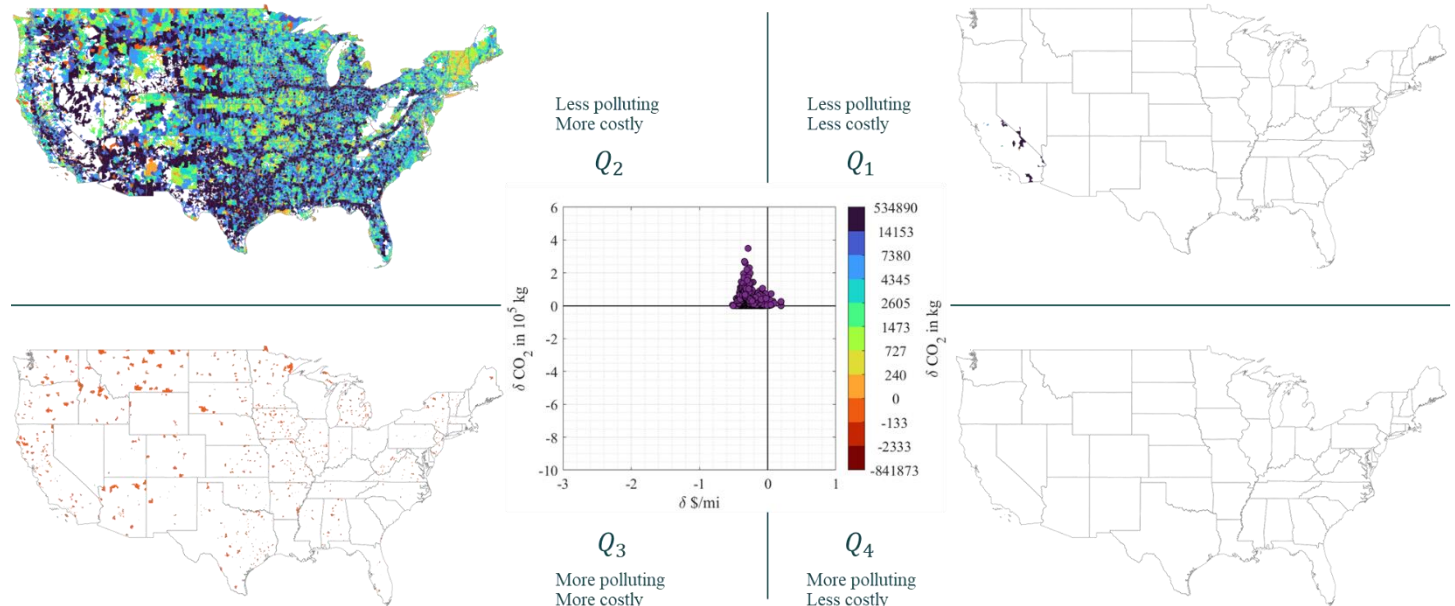


Figure 9. In the center is a scatter plot of the predicted reduction in kg CO₂ emissions (δCO_2) vs. reduction in TCO per mile ($\delta\$/\text{mi}$) of each ZCTA resulting from a transition to *enh. FCEVs* from *enh. diesel HDVs* using electrolytic hydrogen produced from local solar power. Each quadrant has a map of the reduction in kg CO₂ for the data points in that quadrant. The regions scattered throughout the U.S. in orange that occur in both Q_2 and Q_3 have no VMT data (i.e. $VMT = 0$).

points. Table 3 summarizes the designations used for each quadrant in the following discussions.

The scatter plot shows that most regions result in a net reduction in carbon emissions at the expense of increased TCO (i.e. in Q_2), with the exception of a region where both carbon emissions and TCO increase (i.e. in Q_3) and one region with lower carbon emissions and TCO (i.e. in Q_1). Note that areas in orange that are visible in both the maps of Q_2 and Q_3 have a $VMT_x = 0$. The region in Q_1 is in the Nevada desert where diesel prices are excessive reaching $>8\text{ \$/gal}$. The only area in Q_3 with higher carbon emissions, is the eastern part

of the Florida Panhandle. This region results in a predicted increase in carbon emissions due to their heavy reliance on fossil fuels (particularly coal and natural gas) to generate electricity [32]. Looking at the map in Q_2 , the regions with the largest reductions (darkest blue) generally follow interstate corridors from the Eastern States to the Midwest due to the larger VMT_x of the regions with interstates. This trend is not as easily observed in Texas, and Mountain and Western states partially due to the larger size of counties and ZCTAs, resulting in lower spatial resolution. There is, however, a large pocket of high reductions in carbon emissions in the

Pacific Northwest due to the regions adoption of renewable energy, particularly hydro, solar and wind power [32].

If the efficiency of the BEV and diesel HDVs are improved (i.e. considering enh. variants), the scatter plot in the center of Figure 7 contracts compared to Figure 6 with std. variants. This means that the variation in emissions benefits and cost differential are lower. The regional trends in carbon emissions seen in Figure 6 still hold in Figure 7, with the exception that the one region in Q_1 has now moved to Q_2 .

Figure 8 presents the same plot for std. FCEVs using locally produced hydrogen from solar electrolysis compared to std. diesel HDVs. In the scatter plot of Figure 8, there is a larger spread in carbon emissions benefits and the change in TCO has shifted right along the x-axis compared to that observed in Figure 6 and Figure 7. All regions are within Q_1 or Q_2 , with most regions in Q_2 . The few regions in California within Q_1 are the same regions mentioned in the prior discussion on TCO with lower predicted TCO for std. FCEVs than std. diesel HDVs considering the use of locally produced solar electrolytic hydrogen. The analogous scatter plot and quadrant maps for the enh. FCEVs using locally produced hydrogen from solar electrolysis compared to enh. diesel HDVs are presented in Figure 9. Comparing the scatter plot from Figure 9 to Figure 8, there is contraction in the spread of points (both in the cost and carbon emissions directions) associated with improving both FCEV and diesel HDVs efficiency. As a result, a few of the regions in Q_1 have moved to Q_2 .

Table 4. Carbon intensity of FCEVs using various sources of hydrogen. The well-to-wheel carbon intensity for diesel ICE HDVs and BEVs using the U.S. grid mix carbon intensity are provided for reference.

Method	Carbon Intensity		
	Well-to-Use [27] ($\eta_{\text{electrolysis}} = 0.7$)	Well-to-Wheel g CO ₂ /mi (% change w.r.t. std. diesel)	
	kg CO ₂ /gal	Std. Diesel	Enh. Diesel
Diesel ICE	12.07	1860 (0%)	1319.0 (-29%)
	g CO ₂ /kWh	Std. BEV	Enh. BEV
U.S. Mix	386	1111 (-40%)	789 (-58%)
	g CO ₂ /kg H ₂	Std. FCEV	Enh. FCEV
U.S. Mix Electrolysis	21153.9	2821 (+52%)	2000 (+8%)
SMR-RNG	1096.9	146 (-92%)	104 (-94%)
SMR-CCS	3709.2	495 (-73%)	351 (-81%)
Solar Electrolysis	2738.6	365 (-80%)	259 (-86%)
Wind Electrolysis	1597.1	213 (-89%)	151 (-92%)
Nuclear Electrolysis	942.08	126 (-93%)	89 (-95%)

It is important to note that further hydrogen production methods could also result in a well-to-wheel reduction in carbon emissions. A regional analysis of these methods is outside the scope of this paper. However, to highlight the great potential of FCEVs, the well-to-use (I_{FCEV}) from [27] and well-to-wheel ($I_{\text{FCEV}}/\eta_{ij}$) carbon intensities of various hydrogen production methods are summarized in Table 4. The chosen hydrogen production methods are as follows: electrolysis using electricity with the entire U.S. grid mixture of generation sources or U.S. Mix Electrolysis; steam methane reforming (SMR) using renewable natural gas (RNG) or SMR-RNG; SMR with carbon capture and sequestration (CCS) or SMR-CCS; electrolysis using

Page 9 of 14

electricity generated from solar, wind or nuclear, respectively, Solar Electrolysis (previously explored from a regional perspective), Wind Electrolysis and Nuclear Electrolysis.

Lastly the potential cost and carbon emissions benefits of solar power could also be applied to BEVs. We have not explored this here as it would necessitate combining solar power with batteries or other means to ensure the availability of charging throughout a day. This is a direction for future research, with ongoing work exploring solar and other distributed energy resources for HD BEVs [36].

Sensitivity Analysis

To reduce the environmental impact of HDVs, the goal is to realize lower well-to-wheel carbon emissions for alternative powertrains, such as BEVs and FCEVs. However, to drive adoption it is important that these alternative powertrains are at least as competitive from a cost perspective as diesel. Ideally, all regions would be in Q_1 of Figure 6 to Figure 9. To move regions to the right (i.e. reduce the TCO), there are two primary levers: reducing the direct per mile costs (e.g. by reducing the price of either electricity or hydrogen); and reducing the capital investment (e.g. by reducing the cost of the battery or fuel cell). To move regions upwards (i.e. reduce the carbon emissions) there are also two levers: reducing the well-to-use carbon intensity of the fuel for the alternative powertrain (e.g. by reducing the carbon intensity of electricity); and increasing the vehicle efficiency.

The prior subsections explored the impacts of increasing the vehicle efficiency by comparing std. and enh. variants of both BEVs and FCEVs. Further, the impacts of reducing the carbon intensity of electricity are evident in the prior discussion on BEV carbon emissions due to the wide range of carbon intensities across the grid. Here, reductions in the cost of electricity, and the cost of the battery for BEVs and fuel cell (FC) for FCEVs are explored. As the battery costs are provided in \$/kWh, we note that the battery is considered to have an energy capacity of 700kWh. Figure 10 illustrates how changing each of these levers for BEVs individually impacts the % of VMT with lower TCO than diesel HDVs. Note that std. BEVs and FCEVs are compared to std. diesel HDVs and enh. BEV and FCEVs are compared to enh. diesel HDVs.

Figure 10(a) presents the % of VMT with lower TCO than diesel achieved by a given reduction in electricity cost (in \$/kWh). Therein, it is evident that only reducing the cost of electricity is likely infeasible as the electricity cost reduction required is between 0.1 and 0.45 \$/kWh to realize lower TCO when electricity rates range from 0.034 to 0.4 \$/kWh (see Figure 1(b)). This is supported with Figure 10(c), where the majority of regions require a net negative cost of electricity to reach TCO parity with diesel.

Next, Figure 10(b) presents the % of VMT with lower TCO than diesel as a result of reductions in the unit battery cost. A base cost of \$250/kWh and profit factor of 80% are assumed in these calculations. Again, reducing only the battery cost is infeasible as a reduction greater than the base cost of \$250/kWh is required to increase the % VMT with lower TCO than diesel for both std. and enh. BEVs.

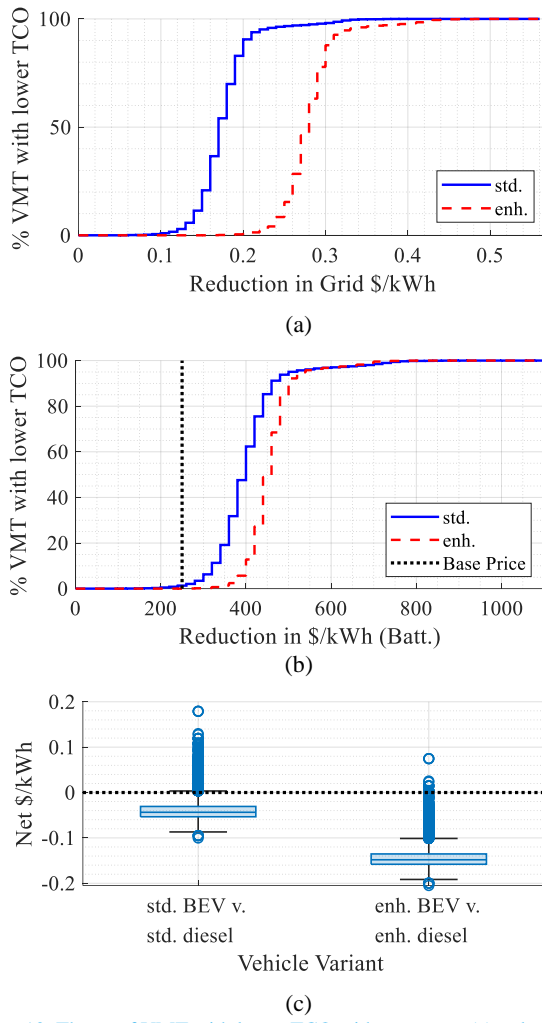


Figure 10. The % of VMT with lower TCO with respect to (a) reductions in grid energy price and (b) reductions in \$/kWh of the battery for BEVs compared to diesel. The net electricity rate for TCO parity with diesel is in (c). The solid blue std. lines compare std. BEVs to std. diesel, and the dashed red enh. lines compare enh. BEV to enh. diesel.

Figure 10 illustrates that a combination of these two levers is required to drive VMT into Q_1 . To illustrate how a multi-pronged approach utilizing reductions in unit battery cost and electricity cost to drive VMT to Q_1 , Figure 11 presents contour plots of % VMT in Q_1 with respect to electricity and battery pricing changes for (a) std. BEVs compared to std. diesel HDVs and for (b) enh. BEVs compared to enh. diesel HDVs. In both Figure 11(a) and (b) electricity rate has a larger impact than battery pricing. However, comparing the contours in Figure 11(b) to those in Figure 11(a), there is a steeper slope, highlighting the increased impact of a reduction in \$/kWh of the battery and reduced impact of a reduction in \$/kWh of electricity for the enh. BEV as a result of increased vehicle efficiency.

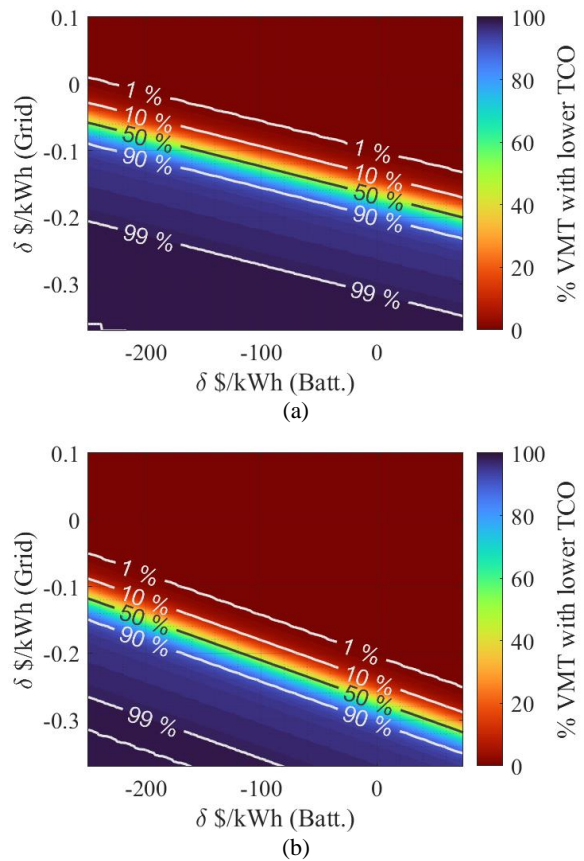


Figure 11. Contours of % VMT in Q_1 for (a) std. BEVs compared to std. diesel and (b) enh. BEVs compared to enh. diesel. The contour line closest to the bottom left corner is the maximum % VMT in Q_1 attainable considering current grid carbon emission intensity.

The analogous plots to those in Figure 10 for FCEVs are presented in Figure 12. A 300kW fuel cell is considered with a baseline cost of the fuel cell considered is \$247/kW. The main differences observed for FCEVs (Figure 12) compared to BEVs (Figure 10) are:

1. reductions in electricity rate (Figure 12(a)) have a more pronounced impact for FCEVs compared to BEVs as hydrogen is a larger portion of the TCO for FCEVs than electricity is for BEVs;
2. as a result of the prior observation, net electricity rates (and therefore hydrogen rates) required for TCO parity with diesel are one average positive with exceptions (Figure 12(c)); and
3. reductions in the cost per kW of the fuel cell for FCEVs has a less significant impact than reductions in \$/kWh of the battery for BEVs, because $C_{rest,FCEV} < C_{rest,BEV}$.

To investigate the combined impacts, contour plots of % VMT in Q_1 with respect to reductions in electricity pricing and unit cost of the fuel cell are given in Figure 13(a) for std. FCEVs and Figure 13(b) for enh. FCEVs. As expected from Figure 12(a) and (b), reductions in electricity rate, and therefore the cost of hydrogen, have a far greater impact than reductions in the cost per kW of the fuel cell.

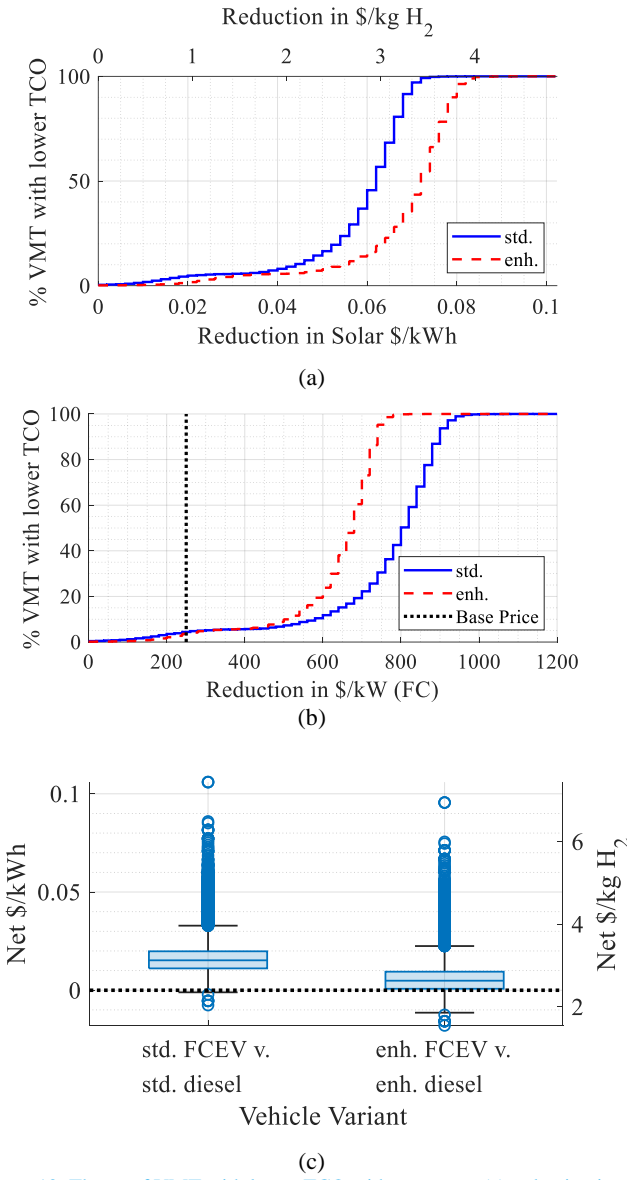


Figure 12. The % of VMT with lower TCO with respect to (a) reduction in grid energy price and (b) reduction in \$/kW of the fuel for FCEVs using electrolytic hydrogen locally produced using solar power compared to diesel. The net electricity rate for TCO parity with diesel are in (c). The solid blue std. lines compare std. BEVs to std. diesel, and the dashed red enh. lines compare enh. BEV to enh. diesel. For reference, the associated reduction in hydrogen cost (\$/kg H₂) is provided at the top of (a) and right of (c).

These analyses have given insights into how the energy pricing and vehicle capital investments need to change in order to realize heavy-duty BEVs and FCEVs that have lower TCO than diesel HDVs. The discussion pertaining to BEVs relies on current data from the grid; however, it omits an investigation into whether the capacity of the grid could support a transition to 100% BEVs. Future work will focus on the grid capacity implications and how the grid may be augmented with distributed energy resources (DER), particularly renewable DER, to compensate for capacity deficits. Furthermore, the regional implications of adding renewable grid capacity for transportation on the associated techno-economic analysis presented in this work will be explored. This work also does not account for limitations of producing hydrogen through solar electrolysis, e.g. only being able to produce during daylight hours and reduced output depending on

Page 11 of 14

cloud cover. Future work will explore a more robust analysis of a wider variety of hydrogen pathways on a regional scale.

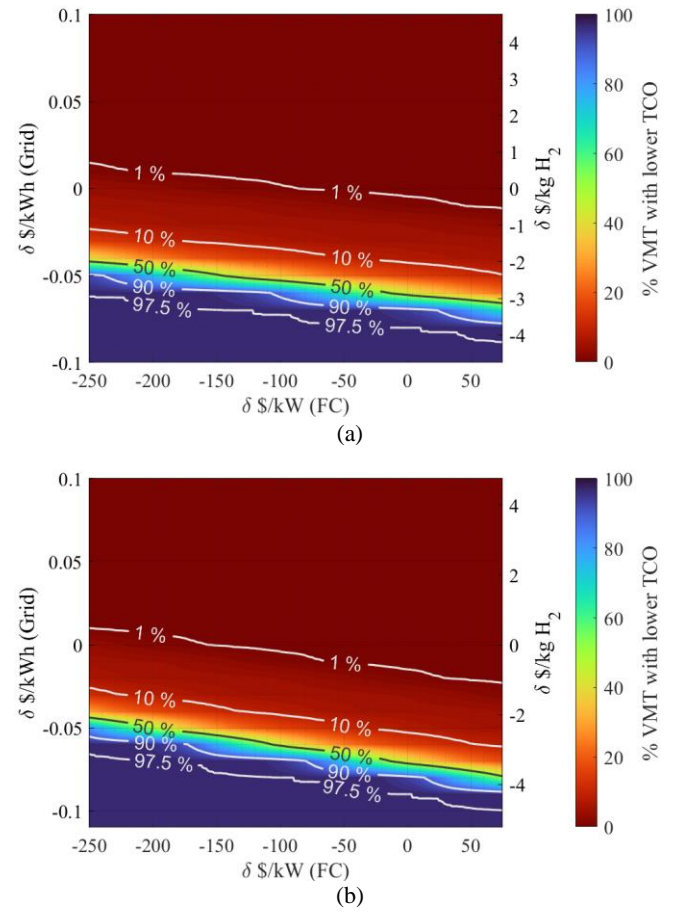


Figure 13. Contours of % VMT in Q_1 for (a) std. FCEVs compared to std. diesel HDVs and (b) enh. FCEVs compared to enh. diesel HDVs. Both FCEV variants are assumed to use electrolytic hydrogen produced locally from solar power. The contour line closest to the bottom left corner is the maximum % VMT in Q_1 attainable due to the lack of data on regional solar energy in some areas (e.g. in parts of the Appalachian Mountains in the eastern U.S. as noted by the white space in Figure 1(e)).

Summary/Conclusions

From the results in the prior section, there are a few important takeaways considering the assumptions made here. Based on the current grid composition and the efficiency of a std. BEV and std. diesel, 0.61% of VMT potentially see an increase in carbon emissions associated with a 100% transition to std. BEVs from std. diesel HDVs. This reduces to only 0.51% of VMT potentially seeing an increase in carbon emissions associated with a 100% transition to enh. BEVs from enh. diesel HDVs. Hydrogen from local solar electrolysis is expected to reduce the carbon intensity for all VMT considering a 100% transition from std. diesel HDVs to std. FCEVs or from enh. diesel HDVs to enh. FCEVs. However, local solar electrolysis is not expected to be widely viable across the nation and our analysis did not account for varying capacity factors of the electrolyzer or the ability and impacts of regional production and distribution. Therefore, it is important to explore alternative production methods (e.g. those in Table 4 of the Results and Discussion section) and distribution/dispensing pathways. This work

is the first step giving a view into where alternative hydrogen generation sources are required, and what regions may be viable for producing hydrogen via local grid or local solar electrolysis (e.g. Washington State for locally produced hydrogen from grid electrolysis or California for locally produced hydrogen from solar electrolysis).

Unfortunately, the BEVs and FCEVs do not provide as significant of an economic benefit compared to diesel HDVs. There are unique regions where alternative powertrains are cost competitive, such as in the Nevada desert where diesel prices are excessive for std. BEVs or scattered throughout California where solar electricity is cheap and diesel prices are high for FCEVs using locally produced hydrogen from solar electrolysis. However, the majority of regions see a TCO premium between 0.30 and 0.6 \$/mi depending on the alternative powertrain and efficiencies being compared. To improve the cost competitiveness of BEVS (both std. and enh.) a balanced approach of reducing electricity costs and capital investment (e.g. the \$/kWh cost of the battery) is required. Conversely, reductions in hydrogen costs are far more important than a reduction in capital investments (e.g. the \$/kW cost of the fuel cell) for an FCEV.

Although, valuable insights are gained from this analysis, the assumptions are limiting. For example, regional variations in elevation, temperature, and vehicle weight/load can have significant impacts on the efficiency of HDVs, therefore future work is focused on estimating variations in HDV efficiency at the zip code level. Other directions for future work include:

- addition of considerations for the required grid improvements to cope with added demand of BEV charging and hydrogen production;
- regional analysis of additional hydrogen pathways beyond local grid electrolysis and local solar electrolysis (e.g. SMR-CCS, etc.), this would include exploring the potential for producing hydrogen in favorable regions and distributing it regionally;
- addition of unexplored costs associated with a transition to alternative powertrains, e.g. the requirement of adding additional parking space for quarantining damaged BEVs;
- incorporation of a regional analysis for the carbon intensity of a gallon of diesel;
- modeling use case considerations, including trip/mission lengths, at a regional level that may restrict the transition or require a single diesel HDV to be replaced by multiple BEVs or FCEVs;
- investigation of the potential benefits from partial adoption of BEVs and FCEVs; and
- exploration of regional changes in criterion emission.

Furthermore, BEVs and FCEVs are not the only alternative powertrains that can reduce carbon emissions compared to diesel HDVs. Future work can expand the regional analysis to consider these additional alternatives, including but not limited to low-carbon fuels (such as, methanol, ethanol, and renewable diesel) for ICE powertrains, hydrogen ICE, or plug-in hybrid electric HDVs.

References

1. O'Dea, J., "Ready for Work: Now Is the Time for Heavy-Duty Electric Vehicles," Union of Concerned Scientists, Cambridge, MA, 2019.
2. Wu, X., Zhou, Y., and Gohlke, D., "Adoption of Plug-in Electric Vehicles: Local Fuel Use and Greenhouse Gas Emissions Reductions Across the U.S.," ANL/ESIA-24/1, Argonne National Laboratory (ANL), Argonne, IL (United States), 2024, doi:10.2172/2314987.
3. Global Memorandum of Understanding on Zero-emission Medium- and Heavy-duty Vehicles, <https://globaldrivetozero.org/mou-nations/>, 2024.
4. Sharpe, B. and Muncrief, R., "Literature review: Real-world fuel consumption of heavy-duty vehicles in the United States, China, and the European Union," The International Council on Clean Transportation, 2015.
5. Vijayagopal, R. and Rousseau, A., "Electric Truck Economic Feasibility Analysis," *World Electric Vehicle Journal* 12(2), 2021, doi:10.3390/wevj12020075.
6. Den Boer, E., Aarnink, S., Kleiner, F., and Pagenkopf, J., "Zero emissions trucks. An overview of state-of-the-art technologies and their potential," 2013.
7. Sen, B., Ercan, T., and Tatari, O., "Does a battery-electric truck make a difference? – Life cycle emissions, costs, and externality analysis of alternative fuel-powered Class 8 heavy-duty trucks in the United States," *Journal of Cleaner Production* 141:110–121, 2017, doi:10.1016/j.jclepro.2016.09.046.
8. Coignard, J., Saxena, S., Greenblatt, J., and Wang, D., "Clean vehicles as an enabler for a clean electricity grid," *Environ. Res. Lett.* 13(5):054031, 2018, doi:10.1088/1748-9326/aabe97.
9. Moulak, M., Lutsey, N., and Hall, D., "Transitioning to zero-emission heavy-duty freight vehicles," The International Council on Clean Transportation, 2017.
10. Chu, K.-C. (Jean), Miller, K.G., Schroeder, A., Gilde, A., and Laughlin, M., "National Zero-Emission Freight Corridor Strategy," 2024.
11. Roeth, M., Park, Y., Schaller, D., Rondini, D., and Ehrenhaft, K., "Executive Summary: 2022 Annual Fleet Fuel Study," North American Council for Freight Efficiency, 2022.
12. Mihelic, R., Schaller, D., Lund, J., Park, Y., Wheeler, J., Otto, K., Brown, J., and Roeth, M., "Run on Less Electric Report: Electric Trucks Have Arrived," North American Council for Freight Efficiency, 2022.
13. H2@UT, "Analysis of Hydrogen Fuel Cell Class 8 Trucks," University of Texas at Austin, 2021.
14. Meijer, M., "Development and Demonstration of Zero-Emission Technologies for Commercial Fleets (SuperTruck 3)," 2024.
15. Bond, E., "Volvo SuperTruck 3: A Zero Emission Freight Future," 2024.
16. Marcinkoski, J., Vijayagopal, R., Adams, J., James, B., Kopasz, J., and Ahluqalia, R., "Hydrogen Class 8 Long Haul Truck Targets," 19006, U.S. Department of Energy, 2019.

17. Sun, R., Sujan, V.A., and Jatana, G., Systemic Decarbonization of Road Freight Transport: A Comprehensive Total Cost of Ownership Model, 2024, doi:10.48550/arXiv.2410.21026.

18. Hunter, C., Penev, M., Reznicek, E., Lustbader, J., Birk, A., and Zhang, C., "Spatial and Temporal Analysis of the Total Cost of Ownership for Class 8 Tractors and Class 4 Parcel Delivery Trucks," NREL/TP-5400-71796, National Renewable Energy Lab. (NREL), Golden, CO (United States), 2021, doi:10.2172/1821615.

19. Alternative Fuels Data Center: Fuel Properties Comparison, <https://afdc.energy.gov/fuels/properties?fuels=GS>, Oct. 2024.

20. GasBuddy - Cheapest Gas Station Finder App with Money Saving Benefits, <https://www.gasbuddy.com>, 2024.

21. National Renewable Energy Laboratory (NREL), U.S. Electric Utility Companies and Rates: Look-up by Zipcode (2023), 2024.

22. US EPA, O., "Energy Attribute Certificates (EACs)," Overviews and Factsheets, <https://www.epa.gov/green-power-markets/energy-attribute-certificates-eacs>, 2024.

23. US EPA, O., "Renewable Energy Certificates (RECs)," Overviews and Factsheets, <https://www.epa.gov/green-power-markets/renewable-energy-certificates-recs>, 2022.

24. Miller, B., Sun, R., and Sujan, V., "Viability Assessment of Wind and Solar Renewable Energy Generation In Support of Nationwide Vehicle Electrification," SAE International, 2025.

25. Maclaurin, G., Grue, N., Lopez, A., Heimiller, D., Rossol, M., Buster, G., and Williams, T., "The Renewable Energy Potential (reV) Model: A Geospatial Platform for Technical Potential and Supply Curve Modeling," NREL/TP--6A20-73067, 1563140, MainId:13369, NREL/TP--6A20-73067, 1563140, MainId:13369, 2021, doi:10.2172/1563140.

26. NREL (National Renewable Energy Laboratory), "2024 Annual Technology Baseline: Equations and Variables in the ATB," https://atb.nrel.gov/electricity/2024/equations_&_variables, 2024.

27. Wang, M., Elgowainy, A., Lee, U., Baek, K.H., Balchandani, S., Benavides, P.T., Burnham, A., Cai, H., Chen, P., Gan, Y., Gracida-Alvarez, U.R., Hawkins, T.R., Huang, T.-Y., Iyer, R.K., Kar, S., Kelly, J.C., Kim, T., Kolodziej, C., Lee, K., Liu, X., Lu, Z., Masum, F., Morales, M., Ng, C., Ou, L., Poddar, T., Reddi, K., Shukla, S., Singh, U., et al., Greenhouse gases, Regulated Emissions, and Energy use in Technologies Model ® (2023 Excel), 2023, doi:10.11578/GREET-Excel-2023/dc.20230907.1.

28. Sujan, V.A., "Understanding Subsidies to Achieve Diesel Powertrain Financial Parity for Heavy-Duty Fuel Cell Electric Vehicles," *SAE International Journal of Sustainable Transportation, Energy, Environment, & Policy (Online)* 4(1), 2022, doi:10.4271/13-04-01-0003.

29. Bureau, U.C., "ZIP Code Tabulation Areas (ZCTAs)," <https://www.census.gov/programs-surveys/geography/guidance/geo-areas/zctas.html>, 2023.

30. Geocorr 2022 - MCDC, <https://mcdc.missouri.edu/applications/geocorr2022.html>, 2022.

31. U.S. Energy Information Administration, "Environment: Carbon Dioxide Emissions Coefficients," https://www.eia.gov/environment/emissions/co2_vol_mass.php, 2023.

32. U.S. Energy Information Administration (EIA), "Open Data," <https://www.eia.gov/opendata/index.php>, 2022.

33. National Renewable Energy Laboratory (NREL), "Life Cycle Assessment Harmonization," <https://www.nrel.gov/analysis/life-cycle-assessment.html>, Mar. 2025.

34. Oak Ridge National Laboratory, Freight Analysis Framework (FAF), 2024.

35. Finlay, J.M., Melendez, R., Esposito, M., Khan, A., Li, M., Gomez-Lopez, I., ..., and Chenoweth, M., National Neighborhood Data Archive (NaNDA): Primary and Secondary Roads by Census Tract and ZIP Code Tabulation Area, United States, 2010 (ICPSR 38585), 2022, doi:10.3886/ICPSR38585.v1.

36. Lucero, J.N.E., Sun, R., Miller, B.A., Onori, S., and Sujan, V.A., A Microgrid Deployment Framework to Support Drayage Electrification, 2024, doi:10.48550/arXiv.2410.01684.

Contact Information

Nathan Goulet
gouletnj@ornl.gov

Acknowledgments

This research used resources of the Compute and Data Environment for Science (CADES) at the Oak Ridge National Laboratory, which is supported by the Office of Science of the U.S. Department of Energy under Contract No. DE-AC05-00OR22725.

This research was supported by the US Department of Energy (DOE) Office of Energy Efficiency and Renewable Energy, Vehicle Technologies Office. The authors thank the support from sponsors and remain solely responsible for the content and opinions expressed. The views and opinions of the author expressed herein do not necessarily state or reflect those of the United States Government or any agency thereof. Neither the United States Government nor any agency thereof, nor any of their employees, makes any warranty, expressed or implied, or assumes any legal liability or responsibility for the accuracy, completeness, or usefulness of any information, apparatus, product, or process disclosed, or represents that its use would not infringe privately owned rights.

Definitions/Abbreviations

BEV battery electric vehicle

CCS	carbon capture and sequestration	SMR-CCS	steam methane reforming with carbon capture and sequestration
enh.	enhanced	SMR-RNG	steam methane reforming using renewable natural gas
FCEV	fuel cell electric vehicle		
HDV	heavy-duty vehicles	std.	standard
RNG	renewable natural gas	TCO	total cost of ownership
SMR	steam methane reforming	VMT	vehicle miles traveled
		w.r.t.	with respect to